Portugaliae Electrochimica Acta 24 (2006) 83-103

PORTUGALIAE ELECTROCHIMICA ACTA

Oxygen Reduction on Polycrystalline Platinum in Alkaline Solution. III. Platinum Surface Modified by Hydrogen Evolution: Additional Data

Carlos Paliteiro,* Elsa Correia

Departamento de Química, Universidade de Coimbra, P-3004-535 Coimbra, Portugal

Received 11 March 2005; accepted in revised form 6 October 2005

Abstract

This paper presents and discusses data collected on the electroreduction of O_2 (ORR) in 1 M NaOH on a polycrystalline Pt surface that initially was pretreated by H_2 evolution at -250 mV in deaerated 0.5 M H_2SO_4 and then evolved with time in a spontaneous and rather slow way towards a full Nekrasov (N-Pt) type behavior, both in the cathodic- and in the anodic potential scan. This fact represents a clear demonstration that a polycrystalline metal surface is a dynamic system and allowed us to carry out the thorough study of the mechanism and kinetics of the ORR on a full N-Pt surface that was not possible in the previous work reported in the Part II of this series. Essentially, we concluded that the change does not alter the ORR mechanism, which is always a series mechanism coupled to disproportionation of the HO_2^- produced; what varies in a given potential range is the value of the rate constants of the different mechanistic steps. It was possible to get absolute values of these constants only for some potential ranges, although the analysis of the data collected provided relative information for the remaining ranges.

Keywords: oxygen reduction, electrocatalytic reduction, physical electrochemistry, metal surface dynamics.

Introduction

A smooth polycrystalline platinum surface of the Nekrasov (N-Pt) type distinguishes from the polycrystalline surface (pc-Pt) resulting from the usual pretreatment based in a series of potential scans between 40 and 1450 mV (potential values referred to the reversible hydrogen electrode, RHE, as all the others mentioned in this paper) by the different way how it catalyses the electroreduction of O_2 in alkaline solution. Such difference is clearly seen when one compares the disc polarization curves obtained in this solution by the

* Corresponding author. E-mail address: paliteir@ci.uc.pt

rotating ring-disc electrode (RRDE) technique. In fact, whereas the polarization curves for the pc-Pt surface show a more or less perfect sigmoidal shape, those for the N-Pt show a current intensity maximum at about 550 mV and a minimum in the 100-200 mV range [1-4]. Simultaneously, the ring current reaches a maximum around 100 mV for the N-Pt surface whereas, for pc-Pt, a rising current intensity is observed at this potential together with a current intensity maximum in the potential range of 750-850 mV [5].

In our previous work [3,4], we showed that it is possible to get the N-Pt surface from pc-Pt after pretreatment of this initial surface by hydrogen evolution at -250 mV in a deaerated 0.5 M H_2SO_4 solution for 10 minutes; following this pretreatment, the pc-Pt surface evolves spontaneously with time to the N-Pt surface. We also reported details of this spontaneous change, stressing in particular that the time needed to complete the change appears to depend from the history of the original pc-Pt surface. In fact, we studied 3 configurations of the final surface that we called A, B and C and, whereas A and B were the end of a fast change (a few days), the evolution that led to C was very slow so that, by the end of two months, we believed to have reached a stable surface. Because of its behavior relatively to the electroreduction of O_2, we then suggested that C was an intermediate between the initial pc-Pt and an N-Pt surface [4].

After this previous work was finished and because work on other subject was done, surface C was kept untouched in a drawer, protected from the contact with the lab atmosphere by a teflon cap, for about one and a half years. When it was finally examined again, it was rather interesting to observe that the evolution process went on along the time up to a true N-Pt surface.

This fact is in itself an interesting result, since it confirms a recent comment made by Burke and co-workers that the redox properties of the metal surfaces and their consequent electrocatalytic activity are variable entities [6]; it also confirmed our suggestion [4] that surface C had an intermediate behaviour between a pc-Pt and an N-Pt surfaces. But without the limitations (pointed out in Ref. [4]) that we faced in the study of surfaces A and B, we decided to carry on a detailed study of the mechanism of the electroreduction of O_2 on this other N-Pt surface called hereafter surface D(N-Pt SD). The results obtained are reported and discussed in this paper.

Experimental details

As mentioned in the previous introduction, the pc-Pt disc / pc-Pt ring rotating electrode (RRDE) used as working electrode was the same used in the Part II of the series [4]. It has a disc geometric area, *A*, of 0.1642 cm^2 and a ring collection efficiency, N, of 0.2202 and was supplied by Pine Instrument. The applied ring potential was 1.08 V. Before use, the disc/ring system was carefully cleaned with ultrapure Milipore-Q water and left overnight dipped in it. Two types of electrochemical cells were used: (i) in the experiments with argon-saturated hydrogen peroxide solutions, a standard three-compartment cell with a Pt-mesh auxiliary electrode separated from the electrolyte solution by a glass frit; (ii) in all the other experiments, a two-compartment cell with a cylindrical, Pt-mesh auxiliary electrode directly dipped in the electrolyte solution around the RRDE,

to prevent the build-up in this solution of hydrogen peroxide formed during the electroreduction of O_2. The cells were first cleaned with a 1:1 solution of 30 % H_2O_2 and concentrated pure NH_3 and washed with Millipore-Q water; when not in use, they were kept immersed in AnalaR concentrated sulphuric acid inside a desiccator.

All solutions were prepared with ultrapure water obtained from Millipore-Q equipment fed with demineralised water irradiated with UV light. The solid NaOH, of proanalysis quality, was supplied by Merck. The 1.065 mM HO_2^- solution mentioned in the next section was prepared, just before its use, by dilution of a 0.238 M solution (concentration obtained by titration with standardised $KMnO_4$ and checked regularly) prepared from a 2 M stock solution of H_2O_2; this stock solution was obtained by dilution of a high purity, non-stabilized, 30 % H_2O_2 solution supplied by Fluka.

Solutions in the electrochemical cells were saturated with high purity O_2 (99.99 %) or argon (99.995 %) from Air Liquide and kept at 25.0 ± 0.1 ºC during the experiments. The potential of the RRDE was controlled by an Ecochemie Autolab (equipped with a PGSTAT 10 potentiostat and a Bipot module and controlled by the GPES 4.8 software). Although the working electrode potential was measured against a AgCl|Ag|3 M KCl electrode with a double junction containing a saturated KNO_3 solution, it is referred in this paper to the reversible hydrogen electrode (RHE). The working electrode rotation was provided by a Pine Instrument AFMSRX rotator.

Results

Reduction of oxygen on N-Pt SD

The polarization disc curves recorded under O_2 saturation, cf. Figs. 1(a) and 1(b), show an N-Pt shape over the entire rotation rate range both for the cathodic and the anodic potential scans. These data were repeatable (i.e., exactly the same data were obtained in a workday) but not reproducible (i.e., they were not exactly the same in different workdays; in fact, the curves shape was practically the same, but minor changes in the current intensity value at a given potential were observed).

Like in all the other polarization disc curves shown below, the plotted current intensity is the measured current intensity subtracted of the blank current intensity at each potential.

We stress the following features of these curves, which were also observed in the polarization curves relative to the reduction of O_2 on N-Pt SA and N-Pt SB (cf. Ref. [4], Fig. 3): (i) the scans show hysteresis, which is particularly noticeable above 1 rps. Above 9 rps, it extends from 40 mV to the onset of the O_2 reduction process and is due to the fact that, in this potential range, the anodic-scan current intensity is higher than that measured in the negative scan, which also makes the onset potential significantly more positive in the anodic scan; (ii) particularly above 4 rps, the curves show a maximum around 600 mV and a minimum in the 150–170 mV range. We also stress that the ring curves of Fig. 1(a) are entirely similar to those observed for surface SB (cf. Ref. [4]).

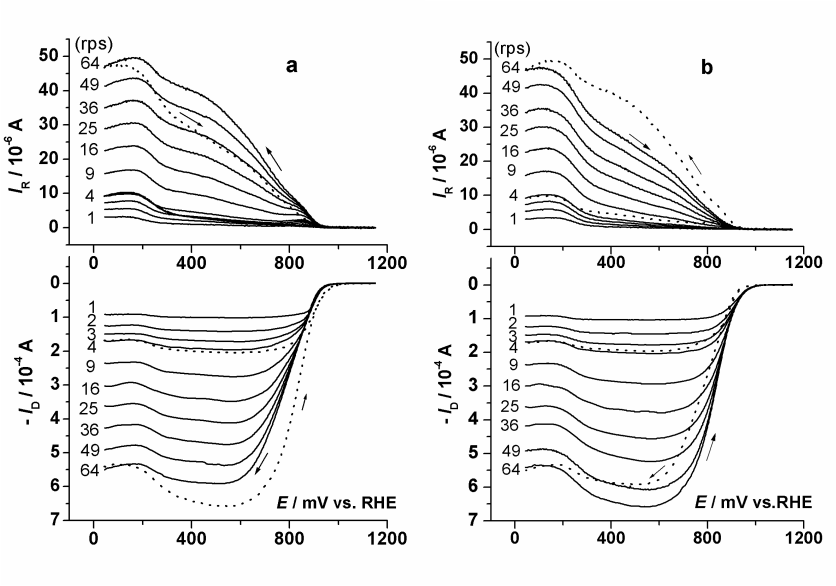

Figure 1. N-Pt SD cathodic (a) and anodic (b) disc polarization curves recorded at 10 mV s^{-1} in O_2-saturated 1 M NaOH. E_{ring} = 1080 mV. A_{disc} = 0.1642 cm^2. (···) Curves for the anodic scan in (a) and for the cathodic scan in (b) recorded in the same experimental conditions at 4 and 64 rps.

The E_D vs. log I_D / [$(I_D)_L$- I_D)] plots (cf. Fig. 2) obtained from the disc polarization curves in Figs. 1(a) and 1(b) using the value of the maximum current intensity as the value of the limiting current intensity, $(I_D)_L$, show two narrow Tafel regions (linear regression parameter not less than 0.997) above 4 rps and only one at and below this rotation rate both in the cathodic- and in the anodic potential scans.

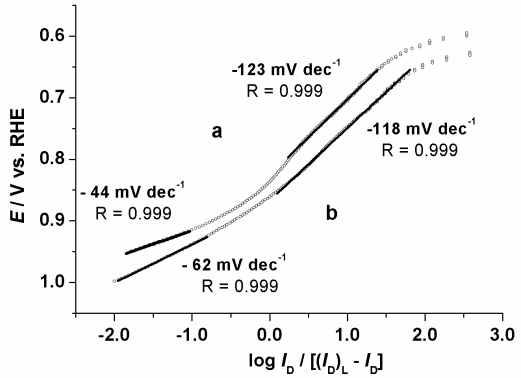

Figure 2. Tafel plots obtained from the curves at 16 rps in (a) Fig. 1(a) and (b) Fig. 1(b).

When we used as the value of $(I_D)_L$ the calculated current intensity at each rotation rate assuming the number of electrons exchanged per O_2 molecule reacted, n, equal to 4, practically the same value of the Tafel slope was obtained

in the lower potential range but no Tafel region was found in the higher potential range.

As found for surfaces SA and SB (cf. Ref. [4]), in the Koutecky-Levich (K-L) I_D^{-1} vs. $\omega^{-0.5}$ plots (where ω is the rotation rate) obtained from the polarization curves of Fig. 1(a), it is possible to distinguish, both for the cathodic (cf. Fig. 3) and for the anodic potential scans, two different shapes which are observed within two different potential ranges.

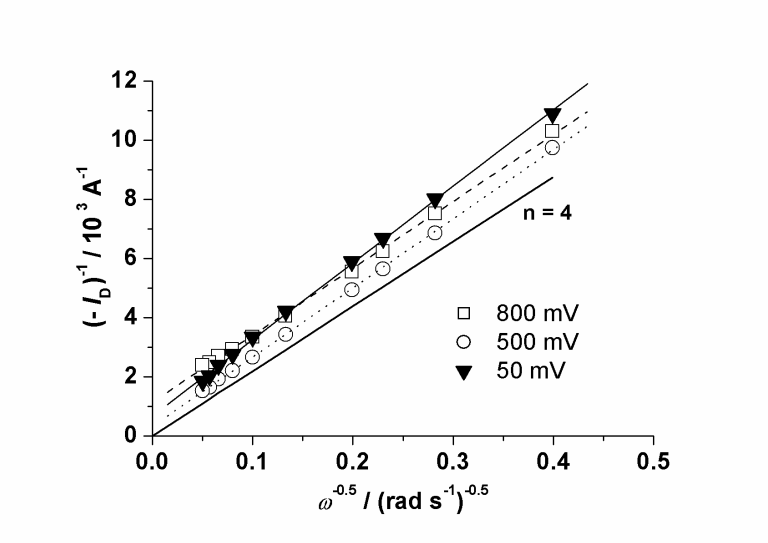

Figure 3. Koutecky-Levich plots obtained from the N-Pt SD anodic polarization curves of Fig. 1(b).

Above 400 mV and below 800 mV, the plots are linear. As mentioned in Ref. [7], this linearity, together with the non-linearity of the plots $I_D^{0.5}$ vs. $I_D\,\omega^{-0.5}$ and I_D^{2} vs. $I_D\,\omega^{-0.5}$, means that the reduction of O_2 on N-Pt SD is a first-order reaction. From the inverse of the slopes, n was calculated from Eq. (1) [8]:

$$(\text{slope})^{-1} = 0.62\, n\, F\, A\, D^{2/3}\, \nu^{-1/6}\, c \qquad (1)$$

where F is the Faraday, A is the electrode disc area, D and c are, respectively, the diffusion coefficient and the concentration of the reacting species in 1 M NaOH and ν is the kinematic viscosity of a 1 M NaOH solution, with F = 96487 C mol^{-1}, $D(O_2)$ = 1.65x10^{-5} cm^2 s^{-1} [9], ν = 1.0624 cm^2 s^{-1} [10] and $c(O_2)$ = 8.4x10^{-7} mol cm^{-3} [11]; the calculated n is shown in Fig. 4 as a function of the electrode potential.

The K-L plot at 800 mV was found to curve up as ω increased, which is an indication of disproportionation of the intermediate HO_2^- ion; the value of n at this potential was therefore calculated from the slope of a straight line fitted to the $\omega < 16$ rps points. The intercepts of the K-L linear plots are never zero, which indicates that the current intensity is never diffusion-controlled.

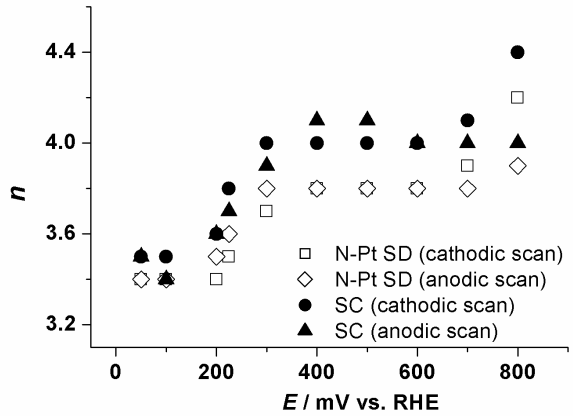

Figure 4. Plot of the number of electrons per O_2 molecule initially reduced as a function of the applied potential.

At and below 400 mV, the K-L plots curve down as ω increases whereas the $I_D^{0.5}$ vs. $I_D\ \omega^{-0.5}$ and the I_D^2 vs. $I_D\ \omega^{-0.5}$ plots are also curved. As pointed out in Ref. [4], these two facts probably indicate that the reduction of O_2 on SD in this potential range is still a first-order reaction but *n* varies with the rotation rate at a given potential in the range. The values of *n* plotted in Fig. 4 for N-Pt SD in this potential range are, therefore, average values calculated from the slope of a straight line fitted to the I_D^{-1} vs. $\omega^{-0.5}$ points.

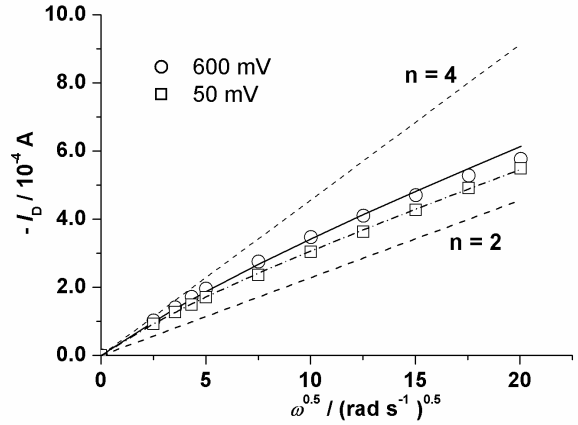

Figure 5. Levich plots for N-Pt SD obtained from the polarization curves of Fig. 1(b). The curves (—) and (–•–) were obtained by fitting Eq. (7) to the experimental Levich plots at 600 mV and at 50 mV, respectively, as explained in the text.

The Levich plots for N-Pt SD (cf. Fig. 5) at and below 600 mV curve down relatively to the calculated 4-electron line as the rotation rate increases.

Reduction of HO_2^- on N-Pt SD

Figs. 6(a) and 6(b) show disc polarization curves recorded on the N-Pt SD immersed in a 1 M NaOH + 1.065 mM HO_2^- solution. In the sense explained above for the data in Figs. 1(a) and 1(b), these data were repeatable but not reproducible.

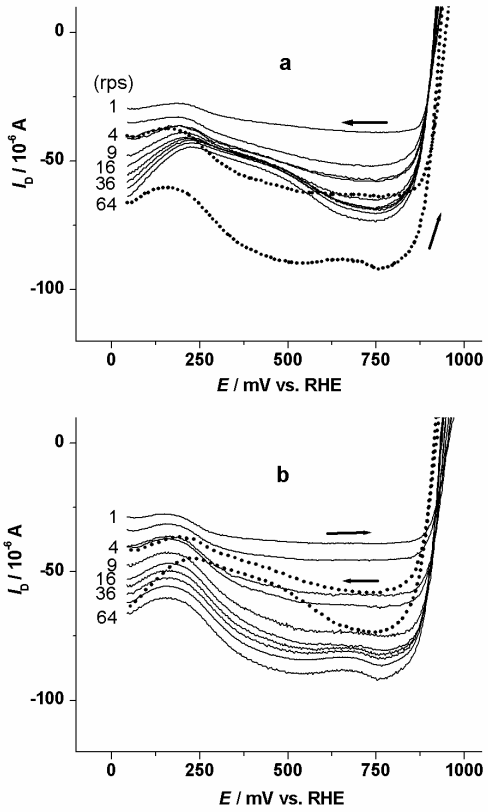

Figure 6. N-Pt SD cathodic (a) and anodic (b) disc polarization curves recorded at 10 mV s^{-1} in argon-saturated 1 M NaOH + 1.065 mM HO_2^-. A_{disc} = 0.1642 cm^2. (····) curves for the anodic scan in (a) and for the cathodic scan in (b) recorded in the same conditions at 4 and 64 rps.

We stress the following details of the HO_2^- reduction curves: (i) a current intensity minimum is observed both in the cathodic- and in the anodic potential scan. The potential of this minimum shifts from 180 to 225 mV as ω increases from 1 to 64 rps in the cathodic scan and has the ω independent value of 155 mV in the anodic scan; (ii) hysteresis between the two scans is noticeable within all the potential range explored; it is particularly significant at the higher rotation rates.

The Levich plots obtained at and below 750 mV for the cathodic and the anodic scans curve down relatively to the calculated 2-electron line as the rotation rate increases (cf. Fig. 7).

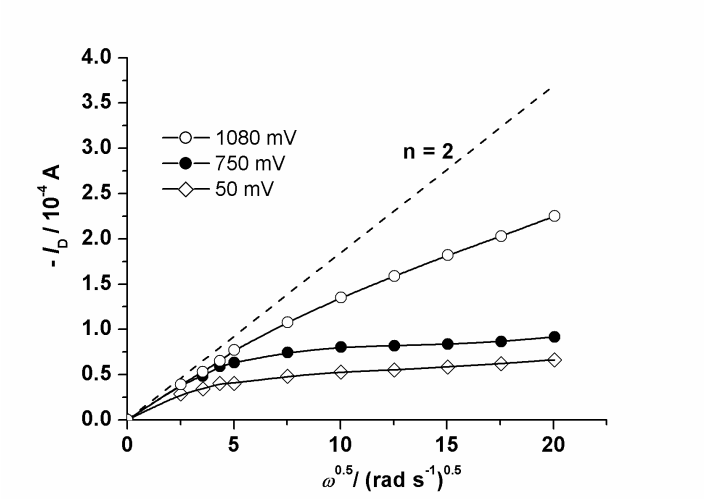

Figure 7. Levich plots for N-Pt SD obtained from the polarization curves of Fig. 6(a).

Tafel regions were found in the polarization curves at low overpotentials, with the slightly rotation-dependent Tafel slopes reported in Table 1.

Table 1. Tafel slopes obtained at 1 rps from HO_2^- reduction polarization curves recorded on N-Pt SD (Figs. 6(a) and 6(b)).

***E* range / mV**	**928-946**	**889-921**	**875-910**	**844-884**	**820-862**
Cathodic scan / mV dec^{-1}		-	-28	-	-72
Anodic scan / mV dec^{-1}	-	-44	-	-59	-

The slopes in this Table were measured in the E_D vs. log I_D / [$(I_D)_L$- I_D)] plots obtained from the curves at 1 rps in Figs 6(a) and 6(b) using the current intensities at 750 mV as values of the limiting current intensity I_L since these currents are practically diffusion-controlled, cf. Fig. 7.

Both in the cathodic and the anodic potential scans, the K-L plots, cf. Fig. 8, are very similar to those found for HO_2^- reduction on SC above 400 mV (cf. Fig. 11 of Ref. [4]). In fact, the I_D^{-1} vs. $\omega^{-0.5}$ points first curve up below 25 rps and then go down as ω increases; the curvature below 25 rps is more intense for N-Pt SD. Below about 300 mV, the curvature gradually decreases and by 50 mV the points are significantly aligned below 25 rps. Therefore, the number *n* of electrons per HO_2^- initially reacted shown in Table 2 was estimated from the linear fitting to the points below 3 rps from 800 to 300 mV, below 4 rps from 300 to 100 mV, below 9 rps at 100 mV and below 25 rps at 50 mV. Eq. (1) was applied in the calculations, with $D(HO_2^-)$ = 8.5 x 10^{-6} $cm^2 s^{-1}$ [12] and $c(HO_2^-)$ = 1.065 mM.

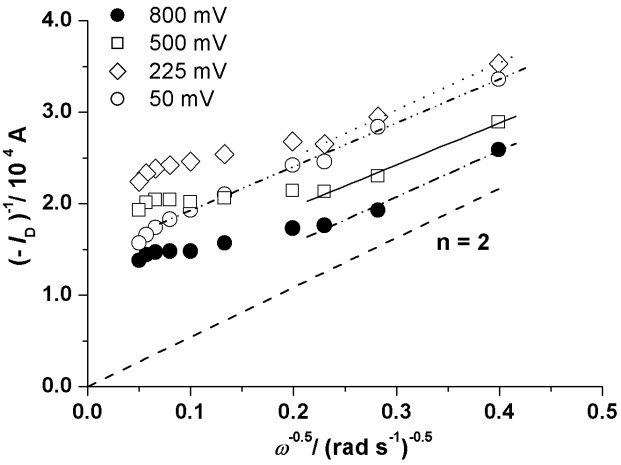

Figure 8. Koutecky-Levich plots obtained from the polarization curves of Fig. 6(a). **(– · –)** and (—) lines fitted to $\omega < 4$ rps points, (····) line fitted to $\omega < 9$ rps points and **(- ·· -)** line fitted to $\omega < 25$ rps points.

Table 2. Average number of electrons per $HO2^-$ initially reduced.

***E* (mV)**	**800**	**700**	**600**	**500**	**400**	**300**	**200**	**100**	**50**
Cathodic scan	2.0	2.0	2.0	2.1	2.1	2.3	2.0	2.2	2.2
Anodic scan	2.1	2.2	2.3	2.3	2.4	2.3	2.3	2.2	2.1

Discussion

Percentage of HO_2^- that diffuses to the solution bulk from surface D

The experimental I_R vs. E_D curves shown in Figs. 1(a) and 1(b) indicate that: (i) both in the cathodic and in the anodic potential scans, in all the potential range explored, the reduction of O_2 produces HO_2^- that does not react further and diffuses, therefore, to the solution bulk; (ii) the amount of such HO_2^- produced clearly depends on the potential and on the direction of the potential scan.

This amount of HO_2^- that diffuses to the solution bulk can be expressed by the following equation:

$$\%\ HO_2^- = \frac{I_R / N}{I_D - I_{blank} + I_R/N} x100 \qquad (2)$$

where I_D, I_{blank}, and N mean, respectively, the disc current intensity in an O_2-saturated solution, the disc current intensity in an argon-saturated solution and the ring collection efficiency. I_R / N represents the value of the disc current

intensity that corresponds to the production of the HO_2^- that diffuses to the solution bulk only if I_R is measured in such experimental conditions that it is diffusion-controlled. This condition was not observed in this work. In fact, the Levich plot for oxidation of HO_2^- taken at 1080 mV (the value of the ring potential fixed in our RRDE experiments) from the disc curves shown in Fig. 6, curves down from the calculated 2-electron line as the rotation rate increases (cf. Fig. 7) and even the measured HO_2^- oxidation current intensity at 1 rps is lower than the corresponding 2-electron current intensity. Also, an even more curved Levich plot was obtained at 1080 mV from the ring polarization curves recorded at 10 mVs^{-1}. This limitation was ascribed to kinetic problems (the oxidation of HO_2^- is slow on Pt oxides that cover the surface at the ring potential [13]) and to the disproportionation of HO_2^- on the ring [14]; its consequence is that the Pt ring is not adequate as a HO_2^- sensor.

Following the same strategy of Ref. [4], we tried to correct the measured values of the ring current intensity by multiplying them by a factor $F = I(n=2) / (I_D)_{1080}$ where $I(n = 2)$ and $(I_D)_{1080}$ mean, respectively, the calculated 2-electron current intensity and the limiting current intensity for the oxidation of HO_2^- on the disc at 1080 mV (the ring potential). Slightly different values of F were calculated in this way for the cathodic and the anodic potential scans. Their averages are presented in Table 3 as a function of the rotation rate.

Table 3. Values of the correction factors F and F_{opt} calculated as explained in text.

rps	**1**	**2**	**3**	**4**	**9**	**16**	**25**	**36**	**49**	**64**
F	1.19	1.41	1.20	1.20	1.27	1.36	1.46	1.54	1.61	1.68
F_{opt}	1.4	1.4	1.4	1.4	1.4	1.5	1.6	1.65	1.65	1.75

Using these values of F to calculate values of the corrected ring current intensity, $(I_R)_{corr}$, we found, at 50 mV, an agreement better than 95% (better than 97 % above 36 rps) between the values of the corrected total disc current intensity, $(I_D)'_{total}$, calculated from the following equation:

$$(I_D)'_{total} = (I_D - I_{blank}) + (I_R)_{cor} / N \qquad (3)$$

(where $(I_R)_{cor}$ means the corrected ring current intensity) and the calculated 4-electron current intensity, $I(n=4)$. However, this good agreement did not extend to the other potentials in the high overpotential range.

Thus, we empirically attempted to adjust the set of F values so that we could keep the good agreement between $(I_D)'_{total}$ and $I(n=4)$ at 50 mV and spread it, consistently, through the high overpotential range at all the rotation rates. The result of that effort is the set of values we call optimum F, F_{opt}, in Table 3. These values of F_{opt} gave an agreement between $(I_D)'_{total}$ and $I(n=4)$ better than 95%

below 500 mV (better than 98 % below 300 mV) between $(I_D)'_{total}$ and $I(n=4)$ at all rotation rates.

The percentage of HO_2^- produced was then calculated by Eq. (2) using values of $(I_R)_{cor} = F_{opt}\, I_R$ instead of I_R and is represented in Figs. 9(a) and 9(b), respectively for the cathodic and the anodic potential scans, as a function of the disc potential.

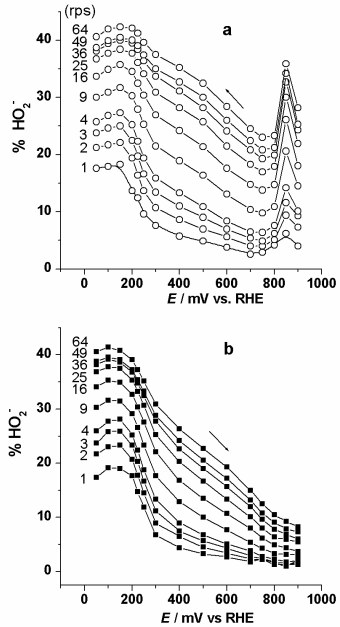

Figure 9. Percentage of HO_2^- that diffused to the solution bulk during O_2 reduction on N-Pt SD as calculated by Eq. (2) with I_{ring} corrected by the F_{opt} values in Table 3. (a) Cathodic and (b) anodic scan.

Mechanism of O_2 reduction on surface D

In Ref. [4] we concluded that O_2 reduction on an N-Pt surface occurs by a series mechanism both in the cathodic and in the anodic potential scans. Above the potential of the minimum (in the configuration of this work's surface, about 170 mV for the cathodic scan and about 150 mV for the anodic potential scan) O_2 is reduced to HO_2^- . This species is then further chemically disproportionated producing O_2 that is recycled below 600 mV giving rise to an enhancement of the current intensity above the 2-electron level. Below 170 mV or 150 mV, respectively for the cathodic and for the anodic potential scan, HO_2^- is further reduced.

We have now more data to support the occurrence of disproportionation. In fact, (i) from the onset of the "reduction" of HO_2^- (≈ 925 mV in the cathodic and ≈ 950 mV in the anodic potential scan) down to the current intensity minimum mV, I_D has a small dependence from the applied potential and the rotation rate (cf. Fig. 6); the Tafel slope below 850 mV is very high; (ii) the HO_2^--"reduction" K-L plots fit the calculated 2-electron line at the lower rotation rates (cf. Fig. 8), but

this line does not cross the origin and the corresponding L plots strongly curve down relatively to the calculated 2-electron line as the rotation rate increases (cf. Fig. 7); (iii) the O_2-reduction L plots curve down relatively to the 4-electron line as the rotation rate increases (cf. Fig. 5). Above 600 mV, the K-L plots curve up at the higher values of the rotation rate relatively to the K-L line fitted to the I_D^{-1} vs. $\omega^{-0.5}$ points at the lower rotation rates (cf. Fig. 3); this fact implies that the number of electrons per O_2 molecule reacted, *n*, decreases as the rotation rate increases at a given potential in the range; (iv) the $(I_D)_L / ((I_D)_L - I_D)$ vs. $\omega^{-0.5}$ plots (where we used the I(n=4) as the value of $(I_D)_L$) from 800 mV (in the cathodic potential scan) or 900 mV (in the anodic potential scan) to about 250 mV show curvature (cf. Fig. 10). This curvature means that the produced HO_2^- on the surface is in equilibrium with the same species in the solution bulk and that, therefore, its concentration on the surface is a function of the rotation rate (decreases when ω increases) [15]; this also implies that, when ω increases, the degree of recycling of the O_2 produced in the disproportionation reaction decreases and that, as a consequence, the measured current intensity decreases. Such a decrease, leads to the decrease as ω increases, implied by the K-L plots, of the number of electrons per O_2 molecule reacted, *n*; (v) the $NI_D / (I_R)_{cor}$ vs. $\omega^{-0.5}$ plots also show curvature from 800 to around 200 mV in both scans (cf. Fig. 11). Such non-linearity occurs if the rate constant for the direct reduction of O_2 to OH^-, K_1, equals zero and the degree of the recycling of O_2 produced in the disproportionation process varies with the rotation rate [16].

We checked if the O_2-reduction L-plots above 200 mV could be fitted by the model proposed by McIntyre [17] to quantitatively describe the limiting current when O_2 is reduced by a regenerative mechanism that involves the disproportionation of HO_2^- catalysed by surface species containing OH according to the following reactions:

$$Pt + OH^- \rightarrow PtOH + e^- \quad (4)$$

$$HO_2^-* + PtOH \rightarrow OH^- + PtO_2H \quad (5)$$

$$PtO_2H + HO_2^- \rightarrow PtOH + O_2* + OH^- \quad (6)$$

where (*) means surface vicinity. The mathematical treatment of the model leads to the following equations [17]:

$$(I_D)_L = 2\,F\,A\,Z_1\,c_1\,\omega^{0.5} + 2\,F\,A\,Z_1\,c_1\,\omega^{0.5}\,[K_4 / (Z_2\,\omega^{0.5} + K_4)] \quad (7)$$

$$(I_D)_L = 4\,F\,A\,Z_1\,c_1\,\omega^{0.5} - (F\,A\,Z_2^2\,\omega / K_4)\,[(1 + 4\,Z_1\,c_1\,K_4 / (Z_2^2\,\omega^{0.5}))^{0.5} - 1] \quad (8)$$

where $Z = 0.62\,D^{2/3}\,\nu^{-1/6}$ and the indexes 1 and 2 refer, respectively, to O_2 and HO_2^-, K_4 is the rate constant for the disproportionation of HO_2^- and the other symbols have the meaning mentioned above (p. 8). According to which one of

reactions (5) and (6) is the slowest, the disproportionation is, respectively, a pseudo first-order reaction (Eq. (7)) or a second-order reaction (Eq. (8)).

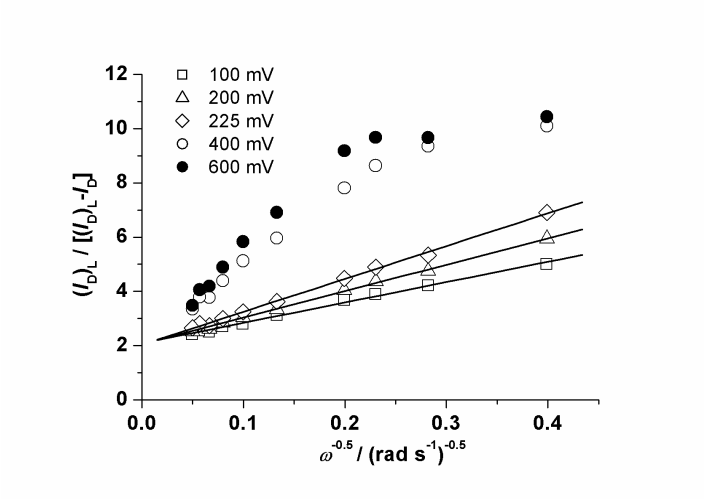

Figure 10. $(I_D)_L / ((I_D)_L - I_D)$ vs. $\omega^{-0.5}$ plots obtained from the disc polarization curves of Fig. 1(b).

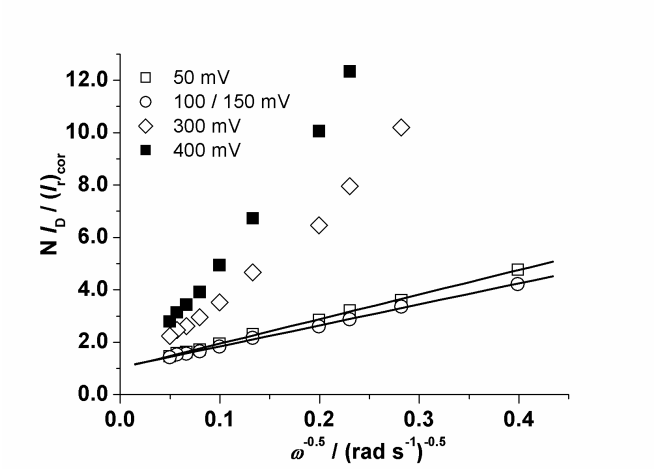

Figure 11. $NI_D/(I_R)_{cor}$ vs. $\omega^{-0.5}$ plots obtained from the disc polarization curves of Fig. 1(b).

To illustrate the application of this model, Fig. 5 shows how the experimental Levich plot at 500 mV, obtained for N-Pt SD from the polarization curves of Fig. 1(b), was fitted by Eq. (7). As the rotation rate increases above 25 rps, the experimental values show a negative shift relatively to the calculated ones. As pointed by McIntyre [17] this happens whenever the rate of removal of HO_2^- from the electrode surface by mass transport becomes significant relatively to K_4, causing the catalytic component of the current intensity to decrease at the higher flux rates. Therefore, the values of K_4 reported in Table 4 were chosen to give the best fit to the experimental current intensities at the lower rotation rates, and the

decision between pseudo-first order and second order disproportionation was based on the best overall fit; pseudo first-order disproportionation always gave the best overall fit. K_4 decreases as the potential goes more negative, which explains why I_D decreases below 600 mV down to about 200 mV.

Table 4. Values of K_4 (in 10^{-2} cm s^{-1}) for HO_2^- disproportionation on pc-Pt, N-Pt SD and SC.

E / mV	**600**	**500**	**400**	**300**	**200**
			Cathodic scan		
N-Pt SD	0.8	0.8	0.8	0.6	0.4
SC [(a)]	1.4	1.3	1.2	-	-
pc-Pt [(b)]	0.8	0.95	1.2	-	-
			Anodic scan		
N-Pt SD	1.4	1.4	1.2	0.85	0.45
SC [(a)]	1.0	0.8	-	-	-
pc-Pt [(b)]	-	-	1.2	-	-

[(a)] Data taken from Ref. [4]; [(b)] data taken from Ref. [5].

The O_2-reduction current intensity is minimum at 170 mV in the cathodic scan (cf. Fig. 1(a)) and at 150 mV in the anodic scan (cf. Fig. 1(b)). These potentials are practically coincident with those at which (i) the ring current intensity reaches a maximum and, simultaneously, (ii) the HO_2^--reduction current also reaches a minimum (cf. Figs. 6(a) and 6(b)). Most probably, at the potential of the minimum the reduction of HO_2^- starts, as was also concluded by Nekrasov and Myuller [1]. This means that, at this potential, the rate constant for HO_2^- reduction, K_3, becomes significant and that, additionally, either K_3 becomes significantly higher than K_4, or K_4 simply turns to zero. The fact that, both in the cathodic and in the anodic potential scan (cf. Fig. 11), the $N I_D / (I_R)_{cor}$ vs. $\omega^{0.5}$ plots are linear below the potential of the minimum with an intercept practically equal to 1, points to $K_4 = 0$ [18]. As it is also $K_1 = 0$, we may write [14]:

$$N I_D / (I_R)_{cor} = 1 + (2 K_3 / Z_2)\, \omega^{-0.5} \qquad (9)$$

From the slope of the $N I_D / (I_R)_{cor}$ vs. $\omega^{-0.5}$ plots and $Z_2 = 5.14 \times 10^{-4}$ cm s^{-1}, it was possible to estimate values of K_3 at 150, 100 and 50 mV; they were, respectively, 2.1×10^{-3}, 2.2×10^{-3} and 2.4×10^{-3} cm s^{-1}.

Influence of the nature of the platinum surfaces on the reduction process

Figs. 12(a) and 12(b) compare the activity towards the electroreduction of O_2, respectively in the cathodic and in the anodic potential scan, of pc-Pt, SC and N-Pt SD surfaces, to characterize the slow pc-Pt to NPt-SD change. The pc-Pt data in these figures were already reported in the Fig. 1 of Ref. [5]. As stressed

there (cf. p. 3437), they were reproducible provided that the upper scan limit was kept above 1200 mV. If that upper limit was fixed below 1200 mV, the current intensity measured in the cathodic scan decreased with repeated scanning and the strong hysteresis then observed in the low overpotential region tended to disappear. The SC data were taken during the work reported in Ref. [4]. We stressed there (cf. p. 3447) that the current intensity measured on a N-Pt surface is stable provided that the upper potential limit is not higher than 1.15 V; it goes back to pc-Pt when we move to more positive potentials. When compared with that described in Ref. [4] (related with a fast change), the pattern of the slow change shows differences in the way how the current intensity evolved at potentials below 500 mV and may correspond to a characteristic pattern of a slow change, confirming SC as a transition surface between pc-Pt and N-Pt. Above 500 mV, the two patterns are practically the same; the change with time of the configuration of the platinum surface in this potential region, leads to a gradual increase of the current intensity and to a shift of the onset of the electroreduction process to more positive potentials. In both cases (fast or slow change), the change ends with a decrease of the current intensity below 600 mV and the formation of a minimum in the 150-200 mV range.
Fig. 13 compares the polarization curves for the reduction of O_2 on the N-Pt SD and the SC surfaces together with the correspondent curves vs. E of the % HO_2^- that is not consumed in the disc at each value of the applied potential, diffuses to the solution and is measured in the ring. Fig. 14 compares normalized polarization curves for the HO_2^- reduction on N-Pt SD and SC. The current intensity was divided by the concentration of the HO_2^- solution used in each case (1.065 mM and 0.99 mM, respectively, in the experiments with the NPt-SD and the SC surfaces).

The analysis of Figs. 13 and 14 leads to the following conclusions: (i) above 600 mV, the current intensity measured on N-Pt SD is consistently greater than that measured on SC both in the reduction of O_2 and in "reduction" of HO_2^-, which suggests that, in this potential range, the value of $K_2 + K_4$ is greater for N-Pt SD than for SC (K_2 means the rate constant for the reduction of O_2 to HO_2^-); (ii) between 600 and 400 mV in the cathodic scan, the current intensity for the reduction of O_2 on N-Pt SD is lower than that measured on SC at all the explored ω values; this is consistent with the fact that, in this potential range, the values of K_4 on N-Pt SD are lower than their corresponding values on SC (cf. Table 4).
However, in the same potential range, the normalized current intensity for the reduction of HO_2^- measured on SC is greater than that measured on N-Pt SD at 64 rps but not at 4 rps; this is only understandable if, in that range, the value of K_2 is lower on SC than on N-Pt SD; (iii) between 500 and 600 mV, in the anodic scan, the relative values of the current intensity measured both for the reduction of O_2 and of HO_2^- are consistent with the relative values of K_4 in Table 4; (iv) below about 400 mV in the cathodic scan and about 500 mV in the anodic scan,

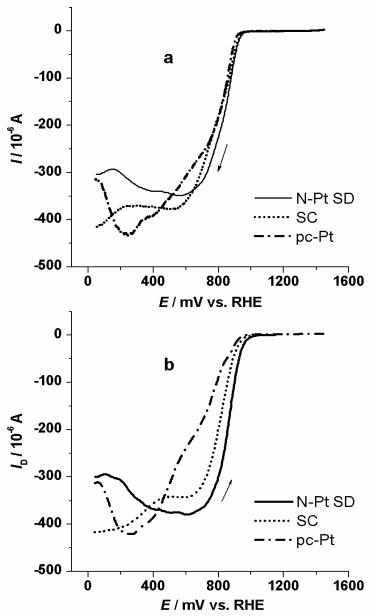

Figure 12. Disc polarization curves recorded at 10 mV s^{-1} and 16 rps in O_2-saturated 1 M NaOH on surfaces N-Pt SD, SC (data taken from Ref. [4]) and pc-Pt (data taken from Ref. [5]). A_{disc} = 0.1642 cm^2. (a) Cathodic scan; (b) anodic scan.

the measured current intensity increases continuously on SC, both for the reduction of O_2 and of HO_2^-; on the contrary, on N-Pt SD the current intensity decreases until about 150 mV (in the cathodic scan) or until about 200 mV (in the anodic scan) and slightly increases after these potentials. Although K_4 decreases continuously both on SC and on N-Pt SD when the applied potential becomes more negative, K_3 becomes dominant on SC below 400 mV in the cathodic scan and below about 500 mV in the anodic scan [4] whereas, as concluded above, on N-Pt SD such dominance only occurs below 150 mV in the cathodic scan and below 200 mV in the anodic scan; these facts may explain the differences between the polarization curves for the reduction of O_2 recorded on SC and on N-Pt SD in the high overpotential region.

We can now summarize what appears to be possible to conclude on the kinetic indicators that characterize the surface change from configuration SC to N-Pt SD: (i) $K_2 + K_4$ increases above 600 mV both in the cathodic and in the anodic scans; (ii) below 600 mV, K_4 decreases in the cathodic scan and increases in the anodic scan; (iii) between 600 and 400 mV in the cathodic scan, K_2 increases; (iv) K_3 strongly decreases below 400 mV in the cathodic scan and below 500 mV in the anodic scan.

Fig. 15 compares the CVs recorded on the pc-Pt (curve 1 in Fig. 1(a) of Ref. [5]), SC (dash curve in Fig. 16 of Ref. [4]) and on the N-Pt SD surfaces. The CV recorded on N-Pt SD is entirely similar to that recorded on N-Pt SA and published in Ref. [4], suggesting that what was then proposed as a model of an

O_2 reduction mechanism mediated by surface species still apply, namely: (i) in the potential regions known as "H sorption" and "OH sorption", the pc-Pt and the N-Pt SD surfaces have different chemical species; (ii) the chemical disproportionation of HO_2^- above 500 mV is mediated by species A_1, A_2 e A_3 (cf. Fig. 15) (where the A species are COH species) according to the following versions of Eq. (4) to (6):

$$C + OH^- \rightarrow COH + e^- \quad (10)$$

$$COH + HO_2^- \rightarrow CO_2H + OH^- \quad (11)$$

$$CO_2H + HO_2^- \rightarrow COH + O_2 + OH \quad (12)$$

with Eq. (11) rate-determining and species A_2 and A_3 more active than A_1 for HO_2^- disproportionation.

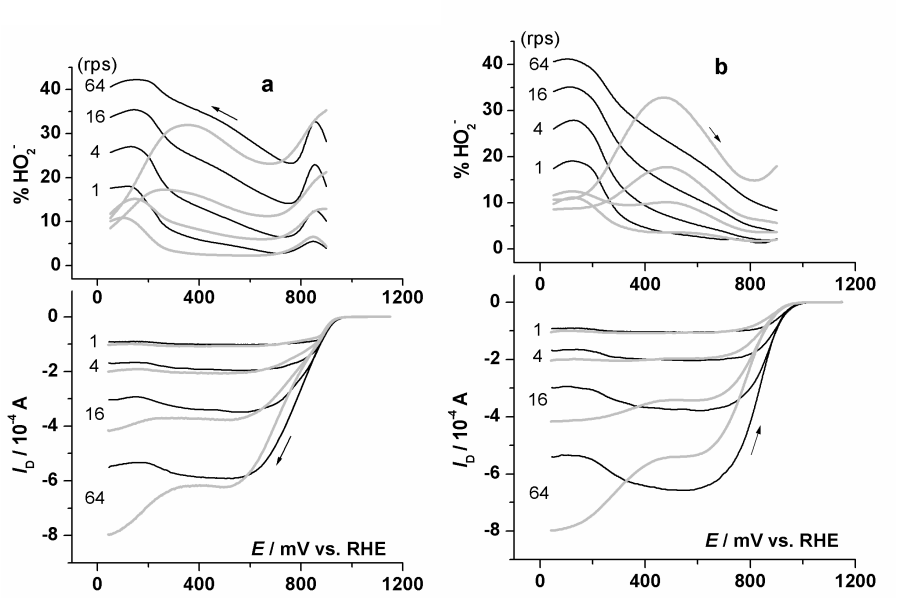

Figure 13. Disc polarization curves recorded at 10 mV s^{-1} in O_2-saturated 1 M NaOH and the correspondent % HO_2^- vs. E curves. A_{disc} = 0.1642 cm^2. (a) Cathodic scan; (b) anodic scan. (—) N-Pt SD curves (data taken from Fig. 1 and Fig. 9 of this work); (—) SC curves (data taken from Fig. 7 and Fig.14 of Ref. [4]).

As already pointed out in Ref. [4], this model needs to be validated with molecular and structural data obtained by *in-situ* spectroelectrochemical techniques, namely *in-situ* XANES (X-ray Absorption Near Edge Structure) and EXAFS (Extended X-ray Absorption Fine Structure), but it has been rather difficult so far to get them. Nevertheless, the clearly observed hydrophilicity of the N-Pt SD surface contrasts with the characteristic hydrophobicity of the pc-Pt surface and is consistent with the existence on it of OH-containing species that may differ from those present on the original pc-Pt surface.

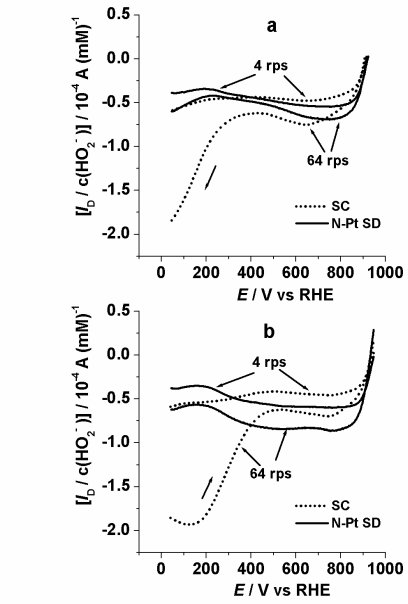

Figure 14. N-Pt SD and SC disc polarization curves recorded at 10 mV s^{-1} and at 4 and 64 rps in argon-saturated 1 M NaOH + HO_2^- and plotted with the disc current intensity normalised to the HO_2^- concentration. A_{disc} = 0.1642 cm^2. (a) Cathodic scan; (b) anodic scan. (—) N-Pt SD (data taken from Fig. 6 of this work); (····) SC (data taken from Fig. 10(a) and Fig. 10(b) of Ref. [4]).

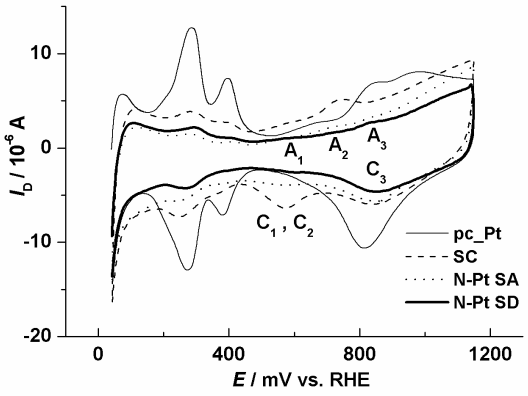

Figure 15. CVs recorded at 50 mV s^{-1} in argon-saturated 1 M NaOH on pc-Pt, N-Pt SA and SC (data taken from Fig. 16 of Ref. [4]), and on N-Pt SD (this work). A_1 to A_3 designate the anodic species of surface redox processes 1 to 3 whereas C_1 to C_3 are their cathodic counterparts.

Conclusions

1. It is possible to trigger a spontaneous change from a "normal" pc-Pt surface to other Pt surface configurations that may have long-time metastability and differ in their electrocatalytic behaviour towards O_2 reduction in alkaline solution. The triggering pretreatment was detailed in p. 3446 of Ref. [4] together with a discussion on its effectiveness and, therefore, can be repeated. Any potential cycling of the changing surface must have an upper limit not higher than 1.15 V, otherwise it quickly returns to the original pc-Pt surface [4].
2. The spontaneous change leads, either quickly [4] or slowly (this work), to a stable N-Pt surface, so called because it was first studied by Nekrasov and Myuller 40 years ago [1,2]. Probably due to a different history, their Pt disc surface responded to the pretreatment by a fast adoption of the N-Pt configuration (this same behaviour was also observed by one of us with the surface N-Pt SB mentioned in Ref. [4]). The detailed work reported in this Part III paper confirms the main conclusions of the Russian workers and supports them with more data and a significantly wider context. At the time, these Russian electrochemists worked at an institute of the Academy of Sciences in Moscow led by Alexander Frumkin. John Bockris wrote recently a few notes on this institute. We stress here the following part of those notes: "For some 20 years, particularly in the 1950s and 1960s, this huge group was at the cutting edge of physical electrochemistry and stimulated much of the post-WWII work in this field in Europe and eventually also in the United States, where its influence was felt on work leading to the fuel cells used in NASA´s early space flights" [19]. If we read the papers published on O_2 reduction by several groups of this institute, we notice, in particular, their strict care with the purification of the solutions they used. Otherwise, it would be quite difficult to get repeatable data collecting them point by point as they did those days.
3. The change process we observed with pc-Pt has close similarities with what can be observed with a "normal" polycrystalline gold (pc-Au) surface; in this case, a mild evolution of H_2 in acid also triggers a spontaneous change from pc-Au to a surface configuration that reduces O_2 in an alkaline solution like a (100) Au surface and was called therefore 100-Au [20,7] (it might, however, be called N-Au since it was also first studied by Nekrasov's group [21]).
4. Compared with the disc current intensity measured at the same potential for the reduction of O_2 on the corresponding pc-Pt surface, that measured on the N-Pt SA and N-Pt SD surfaces is smaller in the high-overpotential region but *greater* in the low-overpotential region (specially in the positive-going scan) (cf. Figs. (1a) and (1b) of Ref. [4] and Fig. 12 of this work); besides, the patterns of the ring currents measured on a N-Pt surface and on the corresponding pc-Pt surface are completely different (cf. Fig. 1 of this work with Fig. 1 of Ref. [5]). It is not possible to explain this behaviour by looking to a N-Pt surface as a contaminated version of a "normal" pc-Pt surface. In fact, Fischer and Heitbaum studied the reduction of O_2 in a pure alkaline solution on a pc-Pt surface configuration similar to ours (similar disc and ring curves) and checked the effect on the reduction process both of the solution contact with air for several hours and of the addition of contaminants to it. They reported that either source of

contamination decreased both disc and ring currents, i.e. decreased the surface activity, from the reduction onset potential down to the potential of H_2 evolution, and did not modify the shape of the disc and ring curves [22].

5. The change from pc-Pt to N-Pt SD (eventually through the hybrid SC configuration) does not alter the ORR mechanism, which is always a series mechanism coupled to disproportionation of the HO_2^- produced; what varies is the value of the rate constants of the different mechanistic steps within distinct potential ranges. These values of the rate constants are apparently influenced by OH-containing surface species of a potential-dependent nature that may act as mediators of the HO_2^- disproportionation and reduction processes that follow the initial reduction of O_2 to HO_2^-. *In-situ* molecular and structural information (eventually provided by the application of *in-situ* spectroscopic techniques like XANES and EXAFS) are therefore needed on this matter but it has been rather difficult to obtain them.

6. By comparing the data reported in this paper with those reported in the previous Part II [4], we were able to find the kinetic pattern of the reduction of O_2 on a slowly-changing Pt surface. On the other hand, it was possible in the Part II work to describe the electrochemical pattern of a fast change. It is evident, therefore, that the processes of the electroreduction of O_2 and of HO_2^- might be used as probes to detect and follow polycrystalline metal surface dynamics.

7. The information obtained in this 3-part study may be rather useful in the detection of a slowly-changing metastable Pt surface, which may be responsible for the occurrence of literature discrepancies. For example, it now becomes clear that the study of the electroreduction of O_2 on polycrystalline Pt in alkaline solution reported by Vilambi and Taylor [23], was carry out on a metastable SC surface (cf. Figs. 2 and 7 of Ref. [23] with Fig. 7(a) of Ref. [4]).

Acknowledgements

We are grateful to the POCTI program (partially funded by FEDER) for financial support (project POCTI / QUI / 35350 / 2000).

References

1. L.N. Nekrasov, L. Myuller, *Dokl. Akad. Nauk SSSR* 149 (1963) 1107.
2. L. Myuller, N. Nekrasov, *Dokl. Akad. Nauk SSSR* 157 (1964) 416.
3. C. Paliteiro, E. Correia, in: S. Hocevar, M. Gabescek, A. Pintar (Eds.), *Electrocatalysis, Advances and Industrial Applications,* National Institute of Chemistry, Slovenia, 1999, pp. 206-208.
4. C. Paliteiro, E. Correia, *J. Electrochem. Soc.* 147 (2000) 3445.
5. C. Paliteiro, L. Batista, *J. Electrochem. Soc.* 147 (2000) 3436.
6. L.D. Burke, J.A. Collins, M.A. Horgan, L.M. Hurley, O'Mullane, *Electrochim. Acta* 45 (2000) 4127.
7. C. Paliteiro, N. Martins, *Electrochim. Acta* 44 (1998) 1359.
8. V.G. Levich, *Physicochemical Hydrodynamics,* Prentice Hall, Englewood Cliffs, NJ, 1962.
9. K.E. Gubbins, R.D. Walker, *J. Electrochem. Soc.* 112 (1965) 459.

10. E.W. Washburn, *International Critical Tables,* Vol. 5, McGraw-Hill, New York, 1929.
11. R.E. Davies, G.L. Horvath, C.W. Tobias, *Electrochim. Acta* 12 (1967) 287.
12. F. Van den Brink, W. Wisscher, E. Barendrecht, *J. Electroanal. Chem.* 172 (1984) 301.
13. C. Paliteiro, A. Hamnett, J.B. Goodenough, *J. Electroanal. Chem.* 233 (1987) 147.
14. H.S. Wroblowa, S.B. Qaderi, *J. Electroanal. Chem.* 279 (1990) 231.
15. V. Vesovic, N. Anastasijevic, R.R. Adzic, *J. Electroanal. Chem.* 218 (1987) 53.
16. A.J. Appleby, M. Savy, *J. Electroanal. Chem.* 92 (1978) 15.
17. J.D.E. McIntyre, *J. Phys. Chem.* 71 (1967) 1196.
18. H.S. Wroblowa, Yen-Chin-Pan, G. Razumney, *J. Electroanal. Chem.* 69 (1976) 195.
19. J.O'M. Bockris, A.K.N. Reddy, M. Gamboa-Aldeco, *Modern Electrochemistry,* Vol. 2A, 2nd ed., Kluwer Academic Publishing, New York, 2000, pp. 1070-1071.
20. C. Paliteiro, *Electrochim. Acta* 19 (1994) 1633.
21. B.G. Podlibner, L.N. Nekrasov, *Sov. Electrochem.* 5 (1969) 308.
22. P. Fischer, J. Heitbaum, *J. Electroanal. Chem.* 112 (1980) 231.
23. N.R.K. Vilambi, E.J. Taylor, *Electrochim. Acta* 34 (1989) 1449.